



1 **Real-time reservoir flood control operation enhanced by data assimilation**

2

3 **Jingwen Zhang<sup>1,2</sup>, Ximing Cai<sup>2</sup>, Xiaohui Lei<sup>3</sup>, Pan Liu<sup>1</sup>, Hao Wang<sup>3</sup>**

4

5 <sup>1</sup> State Key Laboratory of Water Resources and Hydropower Engineering Science, Wuhan  
6 University, Wuhan 430072, China

7 <sup>2</sup> Department of Civil and Environmental Engineering, University of Illinois at Urbana-  
8 Champaign, Urbana, Illinois, USA

9 <sup>3</sup> China Institute of Water Resources and Hydropower Research, Beijing 100038, China

10

11 Corresponding authors: Ximing Cai ([xmcai@illinois.edu](mailto:xmcai@illinois.edu)); Xiaohui Lei ([lxh@iwhr.com](mailto:lxh@iwhr.com))

12

13 **Key Points:**

14 • A human-machine interactive method is proposed for practical real-time reservoir flood  
15 control operation.

16 • Modeling, observation, and operators' experiences are integrated for more effective  
17 decision support for real-time reservoir operation.

18 • Optimization, simulation, and observation are combined for reservoir flood control via  
19 data assimilation for long and narrow reservoirs.

20



21 **Abstract:**

22 Real world reservoir operations are usually not fully automatic based on computer models;  
23 instead, reservoir operators conduct the operations based on their experiences, professional  
24 justification, as well as modeling support for some cases due to unavoidable gap between  
25 computer modeling and real world reservoir operation conditions. In this paper, we propose a  
26 human-machine interactive method, namely Real-time Optimization Model Enhanced by Data  
27 Assimilation (ROMEDA) for reservoirs which have complex storage and stage relations (e.g.  
28 long and narrow reservoirs). The system is composed of 1) an optimization model to search for  
29 optimal releases, 2) reservoir operators' choices based on their experiences, knowledge, and  
30 behaviors, and 3) a reservoir storage-stage simulation and data assimilation schedule to update  
31 the storage based on real-time reservoir stage observations. For every time period and based  
32 on the updated storage, ROMEDA provides optimal releases as recommendations, actual  
33 releases made by operators, as well as a warning of flood risk when the storage exceeds a  
34 threshold level. ROMEDA does not assume that operators strictly accept the recommendations,  
35 and storage will be updated based on actual release at each time period. Via a case study on-  
36 channel reservoir, it is found that for both small and large flood events, ROMEDA, which  
37 integrates the advantages of both machine and human, shows better performance on flood risk  
38 mitigation and water use (hydropower) benefit than the case with historical operation records  
39 (HOR) or optimization with single/multi-objective. ROMEDA is one of the first attempts of a  
40 human-machine interactive method for online use of an optimization model for real-time  
41 reservoir operation based on integrated modeling, observation, and operators' choice.

42



43 **Keywords:** Optimization model, human-machine interactive, data assimilation, reservoir  
44 operation, real-time flood control

45 **Plain Language Summary**

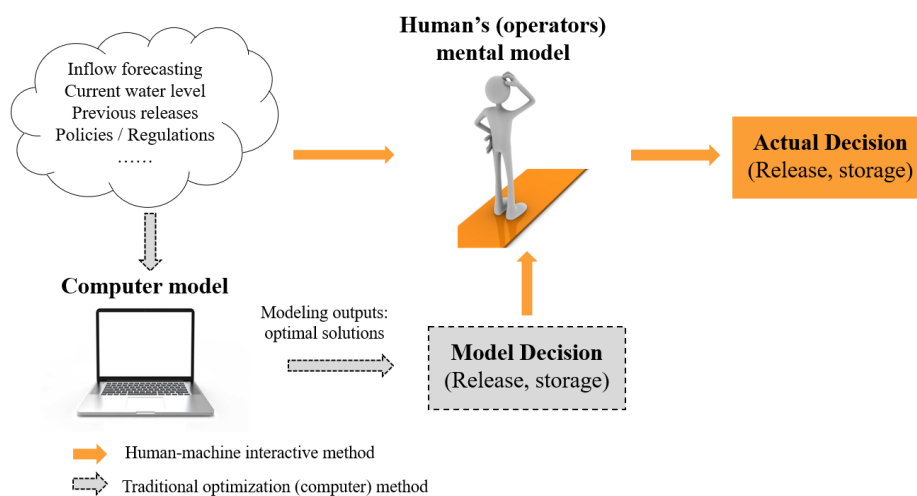
46 Real-time reservoir flood control operation is normally controlled manually by  
47 reservoir operators based on their experiences and justifications, rather than by computer  
48 automatically. Computer models usually are limited in reflecting reservoir operators'  
49 behaviors, thoughts, and priorities at particular times, resulting difficulty in direct use of the  
50 models. In this study, we investigate how to combine machine (computer optimization model)  
51 and human together to make the optimization model useful for real-time reservoir flood control  
52 operation. To do this, a human-machine interactive modeling method is established to combine  
53 computer optimization model, human's consideration, and reservoir stage observations for  
54 actual decisions on release for real-time reservoir flood control operation. Specifically, the  
55 optimization model provides release recommendations and a warning of flood risk; reservoir  
56 operators determine actual release decisions based on their justification and experience based  
57 on optimal release recommendation; however, they must deal with flood risk. To maintain the  
58 actual reservoir storage over time, we use reservoir stage observations to update the reservoir  
59 storage through data assimilation at each period. Via a case study reservoir, we find that real-  
60 time reservoir flood control operation enhanced by data assimilation can reduce the flood risk  
61 and improve water use benefit simultaneously.



## 62 **1 Introduction**

63 Real world reservoir operations are usually not fully automatic based on computer  
64 models; instead, reservoir operators conduct the operations based on their experiences,  
65 professional justification, and modeling support for some cases. This is because of the  
66 unavoidable gap between computer modeling and real world reservoir operation conditions  
67 (Hejazi and Cai, 2011). Especially, at present, models can hardly replace the “mental model”  
68 that is composed of experiences, knowledge, and behaviors of reservoir operators. Computer-  
69 based models for reservoir operations, especially optimization models, are usually used for  
70 “offline” analysis and providing information support for reservoir operators. Thus, it is not  
71 appropriate to assume that a model, no matter how complex it is, can be used for automatic  
72 real-time reservoir operation, although this is often the attempt of modelers.

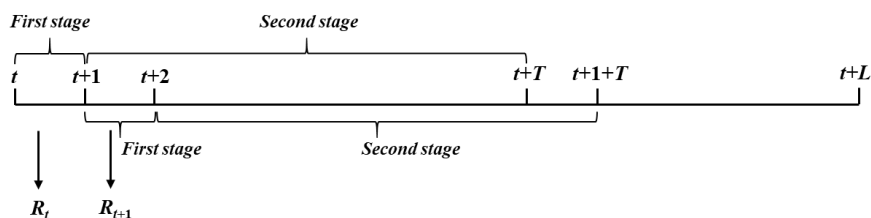
73 In this paper, a human-machine interactive method is presented to support real-time  
74 reservoir operation, using reservoir flood control as an example. By this method, an  
75 optimization model for minimizing flood hazard is used for online reservoir operation via  
76 interactions with reservoir operators, as shown in Figure 1.



77

78 **Figure 1** The schematic of the human-machine interactive method for the online use of a  
79 computer model for reservoir operation

80 Many reservoir operation studies have addressed the problems of real-time optimal  
81 reservoir releases (Becker and Yeh, 1974; Chu and Yeh, 1978; Hsu and Wei, 2007). A typical  
82 real-time optimization model follows a two-stage automatic rolling-over operation scheme as  
83 shown in Figure 2: at each time period ( $t$ ), the model determines reservoir releases at the current  
84 stage and projects releases during the periods of hydrological forecast horizon ( $T$ ), updates the  
85 storage at the end of the period based on the release decision at the current stage, and moves  
86 forward to next time period to conduct the same modeling exercise (You and Cai, 2008; Ding  
87 et al., 2015; Draper, 2001; Draper and Lund, 2004; Zhao et al., 2012). In previous studies, such  
88 a two-stage model runs period by period and assumes that reservoir operators always follow  
89 the release provided by the optimization model at each time period (i.e., automation enabled  
90 by the optimization model).



91

92 **Figure 2** Schematic of real-time two-stage rolling-over operation;  $t$  represents the time step;  $T$   
93 is the forecast horizon (Zhao et al., 2019);  $L$  is the remaining study period of the entire flooding  
94 season.

95 Bauser et al. (2010) proposed that real-time control concept should include three parts:  
96 real-time system simulation model, real-time observations, and optimization algorithm. Real-  
97 time observations can be used to update the system simulation and make them close to reality.  
98 Optimization algorithm can couple the three parts together to deliver optimal control decisions  
99 at a rate in accordance with the response time of the real-time system (Bauser et al., 2010).  
100 Current studies on real-time reservoir operation mostly focus on real-time system models and  
101 optimization algorithms, aiming to explore a normative optimal solution with potential  
102 benefits. How to use observations in real-time control system and make it useful for practical  
103 reservoir operation remains a research challenge (Chang and Chang, 2001; Chang et al., 2005;  
104 Dubrovin et al., 2002; Galelli et al., 2014).

105 The simplest method to incorporate real-time observations into real-time decision  
106 support system is to update the model states by using the real-time observations directly as the  
107 new states. Deng et al. (2015) used observed reservoir stages to estimate the reservoir inflow  
108 by a simple water balance method. However, the procedure can result in inflow fluctuations  
109 and even negative inflow values due to observation error and the uncertainty of the relationship



110 between reservoir storage and stage. This indicates that the direct use of real-time observations,  
111 which ignores the model error and observation error, could lead to the error propagation. In  
112 addition, the direct use of limited real-time observations can only update some but not all  
113 modeling states. If the model is continuous, it is inappropriate to replace only a limited number  
114 of model states using available observations and ignore others. Thus, the direct use of real-time  
115 observations at limited locations or time points may end with significant errors, and combining  
116 observations and modeling is a more effective way to simulate the continuous states of a  
117 process (Crow and Loon, 2006; Huang et al., 2002; Trenberth et al., 2008).

118 Real-time observations are usually incorporated via more sophisticated data  
119 assimilation techniques to improve dynamic modeling, as demonstrated by numerous modeling  
120 efforts in ocean modeling (Evensen, 1994; Carton and Giese, 2008; Oke et al., 2005), weather  
121 forecasting (Kanamitsu, 1989; Houtekamer and Mitchell, 1998; Barker et al., 2004),  
122 hydrological modeling (Xie and Zhang, 2010; Reichle et al., 2008; Wang and Cai, 2008), etc.  
123 Data assimilation has been also applied to the water resources system modeling for more  
124 efficient operation (Bauser et al., 2010; Munier et al., 2015). Bauser et al. (2010) used an  
125 optimal real-time control approach with data assimilation to manage the urban groundwater  
126 well fields to reduce diffuse pollution in the Hardhof field of Zurich, Switzerland. Ensemble  
127 Kalman Filter (EnKF) was applied to incorporate 87 online groundwater head observations  
128 into a three-dimensional finite element subsurface flow model for real-time allocation of  
129 artificial recharge. Munier et al. (2015) applied data assimilation for operational water  
130 management on the upper Niger River Basin. The virtual Surface Water and Ocean  
131 Topography (SWOT) observations of reservoir and river levels with a repeat cycle of 21 days



132 were assimilated to initialize a model predictive control algorithm for optimal reservoir  
133 operation. These studies showed that water resources management supported by the  
134 assimilation of real-time observations outperformed the optimization models without the online  
135 data support.

136 This study utilizes data assimilation to connect reservoir optimization-simulation  
137 models and observations resulting from actual reservoir releases decisions. Many previous  
138 studies on real-time reservoir operation optimization used a simple lumped water balance  
139 model to represent the reservoir dynamics (Galelli et al., 2014), or simply use the observed  
140 stages and the storage-stage relationship to calculate the reservoir storage. In this study we  
141 demonstrate that an unsteady flow routing simulation model is needed for reservoirs that are a  
142 long and narrow channel, for which it is not accurate enough to use a static storage-stage  
143 relationship to simulate the reservoir storage; while it is also impossible to measure the storage  
144 directly because the reservoir surface is not flat. This special case, which exists for many large  
145 and long reservoirs around the world, solicits the use of the data assimilation technique to  
146 enhance the accuracy of the unsteady flow routing model using observed stages at different  
147 sections along the reservoir channel to update model states and also control model and  
148 observation errors.

149 The primary goal of the present paper is to combine the traditional optimization model  
150 (i.e. computer model) and human's consideration together for real use of an optimization model  
151 on real-time reservoir flood control. This paper is to address the following three questions: (1)  
152 How can the computer model and human's consideration be combined for online real-time  
153 reservoir operation? (2) What is the performance of the combined method compared to the



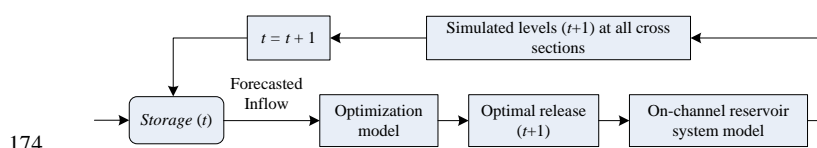


154 actual operation or the result of the optimization model? (3) What is the impact of observations  
155 on the real-time reservoir flood control? To answer these questions, we propose the Real-time  
156 Optimization Model Enhanced by Data Assimilation (ROMEDA) via a human-machine  
157 interactive method with the assimilation of real-time observations. Observed data, reservoir  
158 operators' choices, and computer models will be coupled in the ROMEDA. In the rest of this  
159 paper, we start with an overview of the two methods (ROMEDA method and OPT method)  
160 and detailed introduction of ROMEDA. Then, an example of an on-channel reservoir for flood  
161 control is used to demonstrate ROMEDA. Finally, the discussion on performances and  
162 characteristics of ROMEDA is compared to those of the optimization model and historical  
163 operation records (HOR).

## 164 **2 Methodology**

### 165 2.1 Overview

166 For the real-time rolling-over reservoir operation, the OPT method, i.e. computer  
167 models, determines the optimal releases with the current storage and forecasted inflow at every  
168 time period ( $t$ ) (Figure 3). The optimal release is automatically assumed as the actual release  
169 and taken as input into an on-channel reservoir system simulation model to calculate the stages  
170 at all cross sections of the channel upstream of the dam, based on which, the simulated reservoir  
171 storage is then determined as the initial storage for the next time period. The on-channel  
172 reservoir system model is a one-dimensional (1-D) hydrodynamic model during flood events  
173 in the Preissmann scheme (Preissmann, 1961).

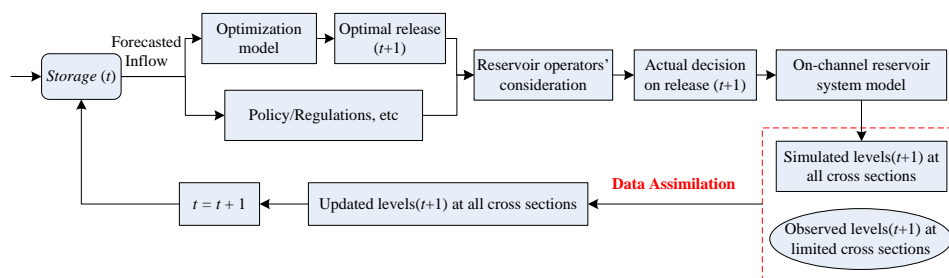


175 **Figure 3** Scheme diagram of the OPTimization (OPT) method

176 The ROMEDA method is illustrated in Figure 4. The real-time optimization model can  
177 provide the optimal releases at each time period of the entire study period. The reservoir  
178 operators can choose to take the result provided by the optimization model or any decision  
179 based on their own priority for the current time period ( $t$ ). At the end of period  $t$ , the reservoir  
180 storage will be updated based on what the operators' choice of reservoir releases and the  
181 optimization model will decide the optimal releases for period  $t+1$  based on the updated  
182 reservoir storage (i.e., the state variable) and the inflow forecast for the rest of the study period.  
183 This procedure will be continued till the end of flooding season. The essential difference  
184 between this method and the direct use of OPT is the online incorporation of 1) reservoir  
185 operators' choices based on their experiences, knowledge and behaviors to determine actual  
186 reservoir releases; 2) the real-time observation of stages along the channel upstream of the dam  
187 to update the reservoir storage so as to provide the optimal release based on actual storage.  
188 Actually, the operators can choose when to adopt the modeling results themselves. This is  
189 because reservoir operators' considerations vary by person and by reservoir. In this paper, as  
190 an illustration example, we set that reservoir operators adopt modeling results when the storage  
191 is over the maximum storage required for leaving space for coming storms. This is only one of  
192 the possible ways of the operators may choose via the human-machine interactive method.



193           A data assimilation method is used to assimilate the observations at some channel  
 194 sections to the on-channel reservoir system simulation model, taking account of both the model  
 195 error and observation error, to update the stages at all cross sections. In this way, the stage  
 196 resulting from the actual decision at time period  $t$  is observed and assimilated to simulate the  
 197 storage at time period  $t+1$ , which is taken as real-time input for the optimization model. Thus,  
 198 compared to the OPT method, ROMEDA provides release decision recommendations for  
 199 reservoir operators period by period and does not assume all the recommendations will be  
 200 adopted by the reservoir operators. In addition, an advanced data assimilation algorithm,  
 201 Constrained Ensemble Kalman Filter with accept/reject method (Wang et al., 2009), to be used  
 202 in the ROMEDA, will handle the impact of both model and observation errors, as detailed later.



203  
 204 **Figure 4** Scheme diagram of the Real-time Optimization Model Enhanced by Data  
 205 Assimilation (ROMEDA) method

206           ROMEDA is similar to Model Predictive Control (MPC) (Garcia et al., 1989; Camacho  
 207 and Alba, 2013; Macian-Sorribes and Pulido-Velazquez, 2019) and other real time control  
 208 approaches, such as on-line adaptive control (Soncini-Sessa et al., 2007), open-loop and closed-  
 209 loop control (Soncini-Sessa et al., 2007; Gerdt, 2012) with respect to more effective use of  
 210 computer-based models and observed data. MPC conducts rolling-horizon optimization based  
 211 on state observations and input forecasts. Essentially, MPC targets a computer-based automatic



212 operation program; while ROMEDA follows the human-machine interactive method. Both  
213 ROMEDA and MPC update the model states using observations at each time step. However,  
214 MPC methods handle predictive environmental disturbance, such as weather forecast  
215 uncertainty (Ficchi et al., 2015; Raso et al., 2014; Maestre et al., 2012); while ROMEDA  
216 integrates operators' choices with the solutions from a computer model. Particularly, MPC  
217 methods usually use the observed data directly; while ROMEDA assimilates observed stages  
218 via a data assimilation technique to update the simulation of reservoir storage. Thus, ROMEDA  
219 couples optimization, simulation, data assimilation, and human choices; the method is tested  
220 with real-time reservoir operation for flood control in this paper.

## 221 2.2 Real-time modeling of an on-channel reservoir system for flood control

### 222 2.2.1 1-D hydrodynamic model

223 The 1-D unsteady flow routing in on-channel reservoir system can be described by the  
224 Saint-Venant equations, including the continuity equation and the momentum equation, as  
225 follows:

$$\frac{\partial A}{\partial t} + \frac{\partial Q}{\partial x} - q = 0 \quad (1)$$

$$\frac{1}{A} \frac{\partial Q}{\partial t} + \frac{1}{A} \frac{\partial}{\partial x} \left( \frac{Q^2}{A} \right) + g \frac{\partial z}{\partial x} - g \frac{n^2 Q |Q|}{AR^{4/3}} = 0 \quad (2)$$

226 where  $A$  is active flow area, i.e. the proportion of the total cross-sectional area with flow;  $Q$  is  
227 the streamflow;  $q$  is the lateral inflow/outflow per unit length, including the runoff generated  
228 along the river channel;  $x$  and  $t$  are the independent variables of space and time, respectively;  
229  $g$  is the acceleration due to gravity;  $z$  is the depth of flow;  $n$  is the roughness coefficient; and  $R$



230 is the hydraulic radius,  $R = \frac{A}{\chi}$ ; and  $\chi$  is the wetted perimeter. The Preissmann implicit four-  
231 point finite difference scheme, a widely used numerical method, is used to solve the 1D  
232 hydrodynamic model (Preissmann, 1961; Castellarin et al., 2009). The streamflow and stages  
233 at all cross sections of the channel upstream of the dam at next time period  $t+1$  can be  
234 determined with the boundary conditions (streamflow at the first and last cross sections, i.e.  
235 inflow and release) at period  $t+1$  and the streamflow and stages at all cross sections at period  
236  $t$ . The water storage between two adjacent cross sections can be calculated as the volume of  
237 prismoid. Thus, the reservoir storage can be determined by accumulating the storage between  
238 all adjacent cross sections. The details of the Preissmann scheme should be referred to  
239 Appendix A.

#### 240 2.2.2 Real-time reservoir optimization model

241 Flood control is the primary objective during the flooding season, and the tradeoff  
242 between the upstream and downstream flooding damage is a longstanding challenge for  
243 reservoir operation. To account for the tradeoff, the real-time reservoir deterministic  
244 optimization model with a short forecast horizon can be set up with a single objective to  
245 minimize the maximum reservoir storage during the forecast horizon (Eq. 3) subject to a  
246 constraint on the maximum release for downstream. However, the reservoir operators'  
247 consideration could go beyond the sole flood control objective even during the flooding season,  
248 and consider to minimize hydropower generation loss during and after the flood control period.  
249 Thus the optimization can also be set up with multi-objectives, i.e., one for flood control and  
250 the other for maximizing hydropower generation (Eq. 4).



$$\min OBJ^* \Leftrightarrow \min [\max S(t)] \quad (3)$$

$$\begin{cases} \min OBJ_1^* \Leftrightarrow \min [\max S(t)] \\ \max OBJ_2^* \Leftrightarrow \max \left[ \sum_t^{t+T} P_t \right] \end{cases} \quad (4)$$

251 where  $\max S(t)$  is the maximum reservoir storage during the forecast horizon ( $T$ ); and  $P_t$  is  
 252 the hydropower generation during time period  $t$ .

253 The major constraints include the lower and/or upper bounds for reservoir release,  
 254 stages at all cross sections, storage, power generation output, and the largest incremental  
 255 release between consecutive time periods:

$$R(t) \leq R_{\max} \quad (5)$$

$$Z_{\min}^j \leq Z^j(t) \leq Z_{\max}^j \quad (6)$$

$$S_{\min} \leq S(t) \leq S_{\max} \quad (7)$$

$$PL(t) \leq P(t) \leq PU(t) \quad (8)$$

$$|R(t) - R(t+1)| \leq \Delta R \quad (9)$$

256 where  $R(t)$  and  $R(t+1)$  are the reservoir releases during time period  $t$  and  $t+1$ , respectively;  
 257  $R_{\max}$  is the maximum allowed release during the flood event;  $Z^j(t)$  is the stage at cross  
 258 section  $j$  for the on-channel reservoir at time period  $t$ ;  $Z_{\min}^j$  and  $Z_{\max}^j$  are the minimum and  
 259 maximum allowed stage at cross section  $j$  for the on-channel reservoir;  $S_{\min}$  and  $S_{\max}$  are the  
 260 minimum and maximum allowed storage for the on-channel reservoir;  $PL(t)$  and  $PU(t)$  are  
 261 the minimum and maximum hydropower generation output limits for the on-channel reservoir  
 262 during time period  $t$ ;  $\Delta R$  is the allowed maximum incremental release over consecutive  
 263 periods.



264 The forecast horizon of the real-time reservoir flood control model is 3 days with a 1-  
265 hour time step. At every time period, the 72 hourly releases during the forecast horizon are the  
266 decision variables. Stochastic global optimization algorithms, Dynamically Dimensioned  
267 Search algorithm (DDS) (Tolson and Shoemaker, 2007) and Pareto archived dynamically  
268 dimensioned search algorithm (PADDS) (Jahanpour et al., 2018), are applied to find the  
269 optimal releases at each time period for a single objective or multi-objective optimization  
270 model (OPT-S and OPT-M). The maximum number of function evaluations with the above  
271 steps is set to 1,000 for every time period by DDS and PADDS. DDS and PADDS can converge  
272 to good solutions rapidly and avoid the poor local optima.

### 273 2.3. Data assimilation

274 Data assimilation techniques can effectively estimate the states of a complex system  
275 with the observations. Ensemble Kalman Filter (EnKF), a sequential data assimilation scheme,  
276 has been widely used in hydrological modeling (Botto et al., 2018; Liu and Gupta, 2007;  
277 Moradkhani et al., 2005; Feng et al., 2017). Two processes, i.e. forecasting and updating  
278 processes, constitute the EnKF framework, described by:

$$Z_{t+1|t}^k = f(Z_{t|t}^k, n) + \omega_t^k, \omega_t^k \sim N(0, W_t) \quad (10)$$

$$Z_{t+1|t+1}^k = Z_{t+1|t}^k + K_{t+1} [Z_{t+1}^{obs,k} - h(Z_{t+1|t}^k)] \quad (11)$$

$$Z_{t+1}^{obs,k} = Z_{t+1}^{obs} + v_{t+1}^k, v_{t+1}^k \sim N(0, V_{t+1}) \quad (12)$$

279 where  $Z_{t|t}^k, Z_{t+1|t+1}^k$  are the  $k^{\text{th}}$  updated ensemble member of the stage vector at time period  $t$   
280 and  $t+1$ ;  $Z_{t+1|t}^k$  is the  $k^{\text{th}}$  forecasted ensemble member of stage vector at time period  $t+1$ ;  $n$  is  
281 the system parameter, i.e. roughness coefficient (see Appendix B);  $f$  represents the system



282 model;  $Z_{t+1}^{obs,k}$  is the perturbed observed stage of selected cross sections of  $k^{\text{th}}$  ensemble  
283 member at time period  $t+1$ , obtained by adding Gaussian observation error  $v_{t+1}^k$  to the  
284 observation  $Z_{t+1}^{obs}$ ;  $h$  is the observation function, i.e. selecting the forecasted stage at selected  
285 cross sections, corresponding to the observations;  $\omega_t^k$  and  $v_{t+1}^k$  are the system model error and  
286 Gaussian observation error, which are assumed to follow Gaussian distribution with zero mean  
287 and specified diagonal covariance matrix  $W_t$  and  $V_t$ . The standard derivation of model state  
288 errors and observation errors are set as 0.5 and 0.01, respectively; and  $K_{t+1}$  is the Kalman gain  
289 matrix.

290 As the forecasted states and updated states may violate the states constraints,  
291 Constrained Ensemble Kalman Filter (CEnKF) is proposed to deal with the violations (Pan and  
292 Wood, 2006; Wang et al., 2009). Because of its computational efficiency and modeling  
293 accuracy, CEnKF with the Accept/Reject Method is used in this paper (Wang et al., 2009). All  
294 constraints in the forecasted and updated states are checked in the forecasting and updating  
295 processes, respectively. A threshold of maximum number of rejections, 500, is set for each  
296 ensemble member at every period to limit the computational burden. If the forecasted/updated  
297 states still violate the constraints when the number of rejections reaches the threshold, the loop  
298 stops, and the states would be set to the boundary directly. The details of the data assimilation  
299 procedures can be referred in Wang et al. (2009).



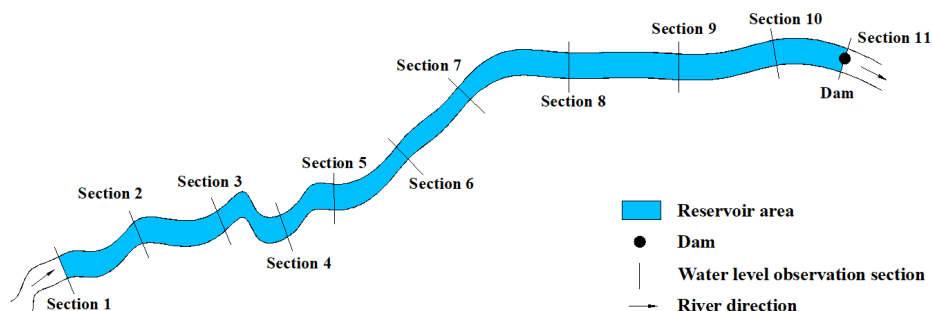


### 300 3 Case study

#### 301 3.1 An on-channel reservoir system

302 An on-channel reservoir for flood control from China is selected to test the proposed  
303 ROMEDA method. The reservoir receives inflow from a drainage area of 56,000 km<sup>2</sup>. The  
304 flood control capacity of the reservoir is 22.2 km<sup>3</sup>. The channel upstream of the dam has a  
305 length of 658 km and the average width of the channel is 1.1 km. Figure 5 shows some selected  
306 sections of the channel. Due to the geometry and topological characteristics (i.e., a long and  
307 narrow channel upstream of the dam), the flood wave propagation requires about 24-36 hours  
308 from the upstream tail of the reservoir to the dam location. The surface of the on-channel  
309 reservoir featured by a significant slope cannot be treated as flat during the flooding season.  
310 Thus, it is not appropriate to simulate the reservoir flood routing by static storage-stage  
311 relationship assuming a flat surface. A 1-D unsteady flow routing model is used to simulate  
312 flood routing in the on-channel reservoir, by which the dynamic reservoir storage is calculated  
313 using a numerical method. Figure 6 shows the longitudinal profile of the bottom elevation of  
314 296 cross sections in the upstream channel of the dam, as well as the reservoir surface. Stage  
315 observations can be obtained from 11 sections as shown in Figures 5 and 6. The characteristic  
316 parameters of the on-channel reservoir are listed in Table 1. It should be noted that hydropower  
317 generation is one of the major functions of the on-channel reservoir, with an installation  
318 capacity of 22,400 MW.

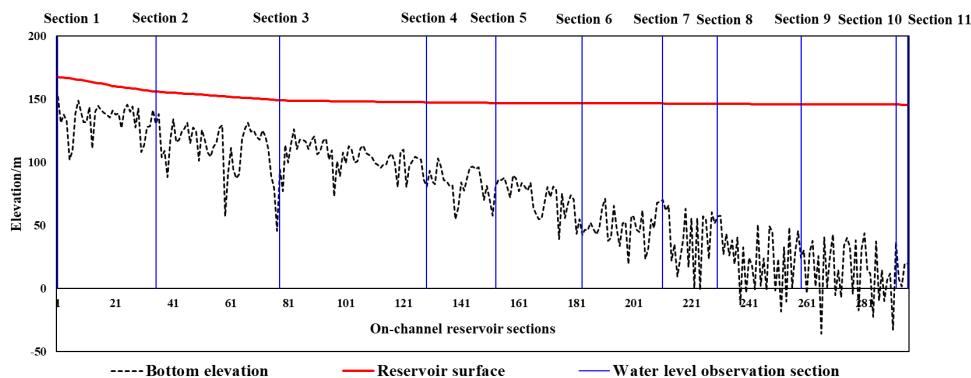
319



320

321 **Figure 5** Schematic diagram of the river and on-channel reservoir

322



323

324 **Figure 6** Longitudinal profile of the on-channel reservoir

325

326 **Table 1** Characteristic parameters of the on-channel reservoir

Flood limited stage (m)	Normal stage (m)	pool (m)	Crest elevation (m)	Flood protection storage (km <sup>3</sup> )	Total reservoir storage (km <sup>3</sup> )
145	175	185	22.15	39.3	

327

### 3.2 Data

328

329

330

Two historical flood events with different magnitudes (small and large) with a time step of 1 hour are selected for case studies. Since the forecast horizon of the real-time reservoir flood control model is set to be 3 days with a 1-hour time step, the forecast uncertainty is



331 relatively low, historical inflows are used as perfect inflow forecast without uncertainty. The  
332 stage observations at the 11 observation sections (Figure 6) are provided with the same time  
333 step (1 hour) during both the small and large flood events. The real-time stage observations  
334 provided to ROMEDA for the case study use the historical stage records resulting from actual  
335 releases during the periods when reservoir operators do not adopt the results from OPT;  
336 otherwise “virtual stage observations” resulting from the OPT suggested releases (adopted by  
337 the operators) are used. The maximum allowed release of the on-channel reservoir during the  
338 flooding season varies depending on the flood magnitudes. In this paper, the maximum allowed  
339 releases for small and large flood events are set to 29,800 m<sup>3</sup>/s and 43,300 m<sup>3</sup>/s, respectively.  
340 The storage threshold for flood risk is 22.8 km<sup>3</sup>.

#### 341 **4 Results**

342 The performance of OPT-S, OPT-M, ROMEDA, and the historical operation records  
343 (HOR) on flood risk and water use benefit are compared in the section. During the flooding  
344 season, the reservoir operators are required to follow the optimal operation aiming to reduce  
345 the flood risk; meanwhile they may have other considerations, such as considering the  
346 maximum allowed flow specified by the hydropower installation capacity to reduce spill. Due  
347 to complex and variable human’s considerations, we test a particular case for simplicity but  
348 without losing generality, i.e., reservoir operators do not necessarily follow the recommended  
349 releases when the current reservoir storage is lower than the storage threshold for the case  
350 reservoir (22.8 km<sup>3</sup>), but will do it when the storage exceeds the storage threshold.



351 4.1 Operation processes

352 The modeling results from the three methods (OPT-S, OPT-M, and ROMEDA), along  
353 with the historical operation records (HOR), are compared in Figure 7 for a small flood event  
354 and Figure 8 for a large flood event. The maximum releases under all these cases reach to the  
355 maximum allowed release ( $29,800 \text{ m}^3/\text{s}$  for a small flood event and  $43,300 \text{ m}^3/\text{s}$  for a large  
356 flood event). OPT-S, driven by the objective of minimizing the peak storage during a flood  
357 event, releases more water to reserve a large flood control storage for future possible flood  
358 events. Under OPT-M, the releases are slightly smaller than that of OPT-S before the flood  
359 peak, which is driven by the objective of maximizing the hydropower generation. As shown in  
360 Figure 7, before the arrival of the first flood peak (during the first 150 time periods in Figure  
361 7a), the releases of OPT-S and OPT-M are larger than those of HOR (but smaller than the  
362 maximum allowed release,  $29,800 \text{ m}^3/\text{s}$ ). Given the forecast of the first and second coming  
363 inflow peaks, the OPT-S and OPT-M releases increase sharply and reach to the highest allowed  
364 level during period 150-180. After the arrival of two flood peaks, the OPT-S and OPT-M  
365 releases, though lower than the maximum allowed release, can make the reservoir storage lower  
366 than the threshold level during all modeling periods.

367 As stated above, the reservoir operators' consideration could go beyond the sole flood  
368 control objective, as avoiding hydropower generation loss during and after the flood control  
369 period is also of concern. Consequently, they may release less water than OPT-S and OPT-M  
370 prescribes to reserve a larger water storage that is beneficial for hydropower generation. As  
371 shown in Figure 7b, rather than a sharp increase ( $500 \text{ m}^3/\text{s}$  per hour) under OPT-S and OPT-  
372 M, the HOR releases during periods 120 to 230, only gradually increase ( $170 \text{ m}^3/\text{s}$  per hour),

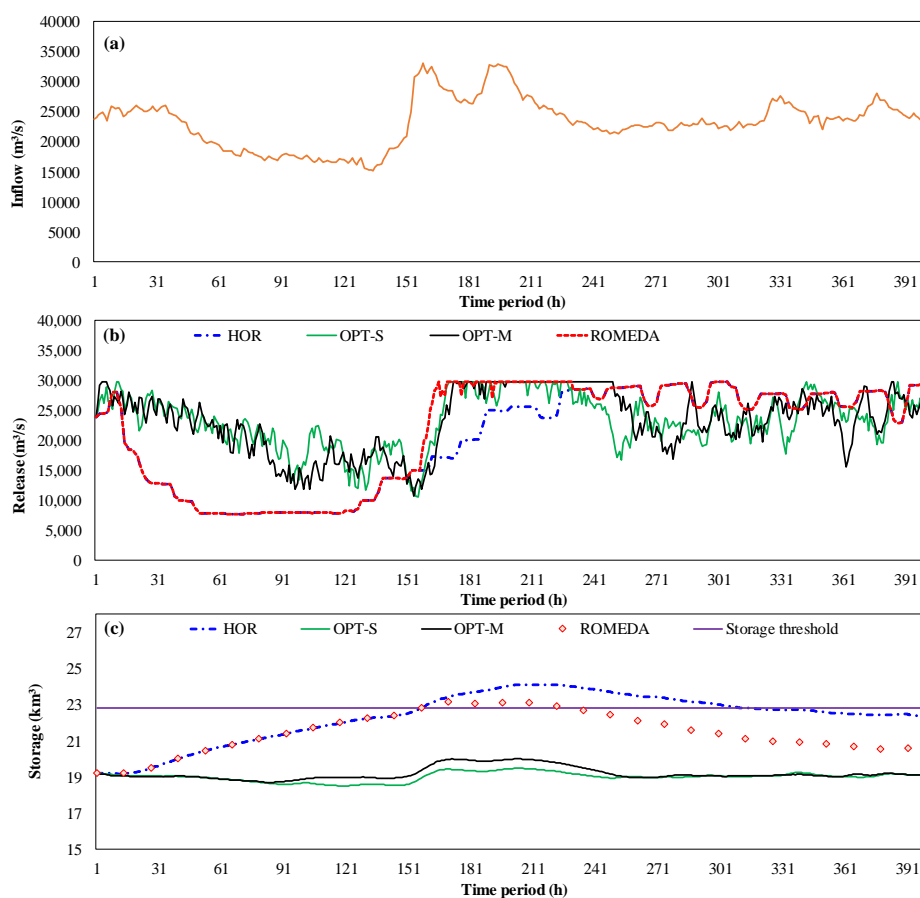


373 which eventually ends with a reservoir storage that exceeds the storage threshold. During the  
374 flood peak period, the HOR release is high but smaller than the maximum allowed release  
375 (while the OPT-S and OPT-M releases approximately equal the maximum allowed release),  
376 which makes the storage under HOR continuously remain above the storage threshold (Figure  
377 7c). After the peak period (period 230 and further), the HOR releases approximately reach the  
378 maximum allowed release to reduce the flood risk since the reservoir storage is still above the  
379 threshold. In summary, the real-world situation (HOR) could be complicated by several  
380 conditions: first, they might take a certain level of risk of flooding for the benefits of  
381 hydropower (i.e., dealing the tradeoff). Second, the operation of the reservoir does not exactly  
382 follow the flood control requirements (i.e., the storage is over the threshold during some  
383 periods). Third, the actual releases might also be affected by the requirement of the maximum  
384 allowed releases to downstream.

385 As assumed, the releases of ROMEDA are basically the same as those of HOR to  
386 maintain water use benefits, when the reservoir storage does not exceed the storage threshold.  
387 The reservoir storage of ROMEDA is updated with the assimilation of real-time reservoir  
388 observed stages, which can mitigate the model error from the 1-D hydrodynamic model. When  
389 the reservoir storage, updated via ROMEDA, exceeds the storage threshold, the reservoir  
390 operators follow the recommended releases from the optimization model in order to reduce the  
391 flood risk. This ends with a large increase of the releases compared to those before the storage  
392 reaches the threshold since the recommended release is close to the maximum allowed release.  
393 By doing that, the reservoir storage of ROMEDA is decreased to the threshold during the flood  
394 peak. After the flood peaks, when the storage is below the threshold, the releases of ROMEDA



395 come back to the HOR releases (after period 230). Due to the impact of peak-clipping  
396 conducted during the flood peak periods, the reservoir storage of ROMEDA is lower than that  
397 of HOR with the same reservoir release after two flood peaks (Figure 7c). Overall, ROMEDA  
398 reduces the flood risk with large releases from the optimization model and meanwhile increases  
399 the hydropower generation from the HOR (see more discussion in the following).



400  
401 **Figure 7** Reservoir operation results of HOR, OPT-S, OPT-M, and ROMEDA four cases for a  
402 small flood event (a) inflow; (b) release, ROMEDA denotes the adopted release in ROMEDA  
403 case; and (c) storage, ROMEDA denotes the updated storage in ROMEDA case



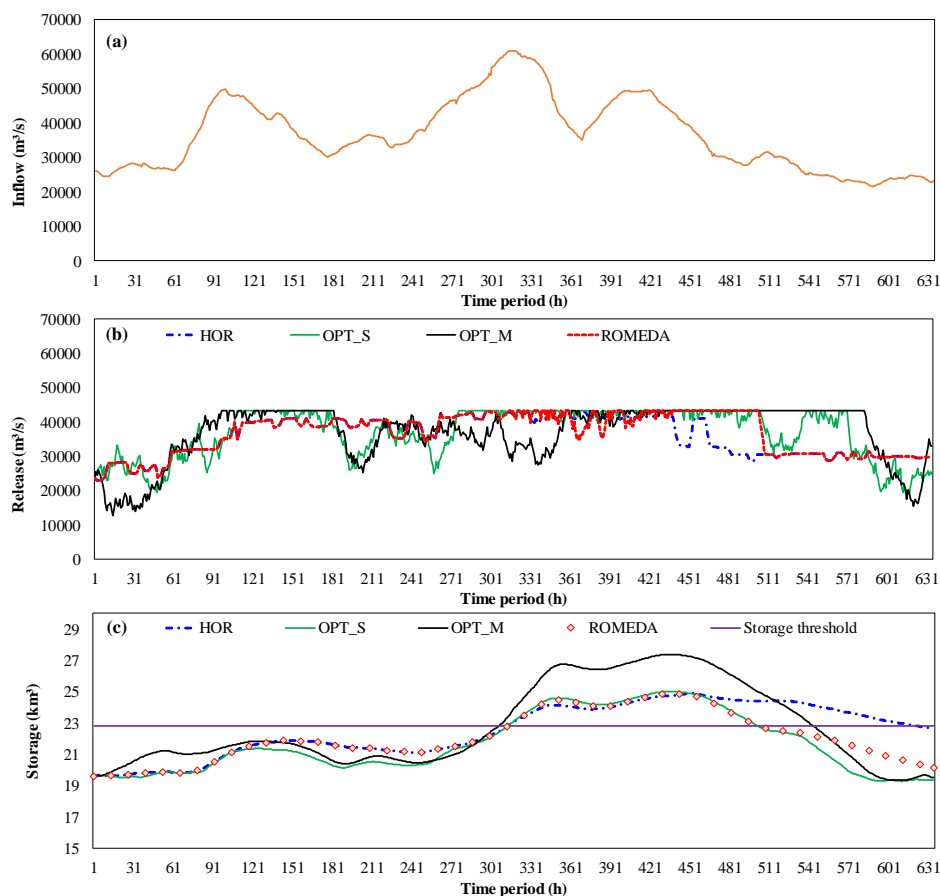
404 Reservoir operation results of the four cases (HOR, OPT-S, OPT-M, and ROMEDA)  
405 for a large flood event are compared in Figure 8. There are three flood peaks in this flood event.  
406 During the first peak, OPT-S releases more water than HOR to reserve the flood control storage  
407 for possible flood peak in future, resulting in smaller reservoir storage under OPT-S than HOR;  
408 while OPT-M releases less water to increase the reservoir storage for larger hydropower  
409 generation. HOR releases increase to the maximum allowed flow specified by the hydropower  
410 installation capacity before the first flood peak, aiming to reduce spill during the flood peak  
411 periods. It seems that the HOR releases correspond to the inflow variability and the reservoir  
412 storage is within the storage threshold though it is higher than those of OPT-S and OPT-M.  
413 After the first flood peak, the HOR releases keep close to the maximum allowed release; while  
414 the OPT-S and OPT-M releases exhibit variations due to the sensitivity to the flood forecast  
415 (noted that the variations can also be caused by the uncertainty of the optimal solution from the  
416 DDS and PADDs algorithms). It is found that the reservoir storage of OPT-S and OPT-M  
417 exceed that of HOR during the second flood peak. Meanwhile, for both HOR and OPT-S, the  
418 releases are close to the maximum allowed release ( $43,300 \text{ m}^3/\text{s}$ ) and the reservoir storage  
419 exceeds the threshold, but OPT-M releases are smaller than the maximum allowed release due  
420 to objective of hydropower generation. After the second flood peak, the storage of both OPT-  
421 S, OPT-M, and HOR still remains above the storage threshold for some periods, but HOR  
422 gradually reduces the releases to the maximum allowed flow designed for the installation  
423 capacity of the hydropower station; while OPT-S and OPT-M keeps the releases at the  
424 maximum level for longer periods. Thus, OPT-S and OPT-M have less periods with its storage  
425 above the threshold and accumulated value of flood risk than HOR (see more discussion in



426 Section 4.2). Overall, compared to a small flood event, HOR, OPT-S, and OPT-M respond to  
427 inflow variability closely during a large flood event, and both end with some periods with  
428 storage over the threshold level. OPT-M has the largest value of maximum reservoir storage.  
429 Meanwhile the HOR releases and storage still imply some considerations beyond flood control.

430 Before period 310, the reservoir storage of ROMEDA is below the storage threshold,  
431 and the ROMEDA releases are the same as those of HOR. After that ROMEDA takes the  
432 recommended releases from the optimization model during the period from the second flood  
433 peak to the end of the third flood peak, during which the ROMEDA storage is over the threshold  
434 level too but having a smaller number of periods with its storage above the threshold than HOR  
435 and OPT-M. After the three flood peaks, the ROMEDA releases come back to the releases of  
436 HOR, and the ROMEDA storage is larger than that of OPT-S and smaller than that of HOR,  
437 which shows a balance of flood control and hydropower generation.





438

439 **Figure 8** Reservoir operation results of HOR, OPT-S, OPT-M, and ROMEDA four cases for a  
440 large flood event (a) inflow; (b) release, ROMEDA denotes the adopted release in ROMEDA  
441 case; and (c) storage, ROMEDA denotes the updated storage in ROMEDA case

442 As shown in Figure 7b, under the small flood event, the HOR releases increase from  
443 the minimum to the maximum taking 110 periods (from period 120 to 230), accounting for  
444 28% of the total periods; the maximum release remains 170 time periods (from period 230 to  
445 400), 43% of the total periods. However, under the large flood event, HOR only takes 70 time  
446 periods (11% of the total flood periods) to increase from the minimum to the maximum release



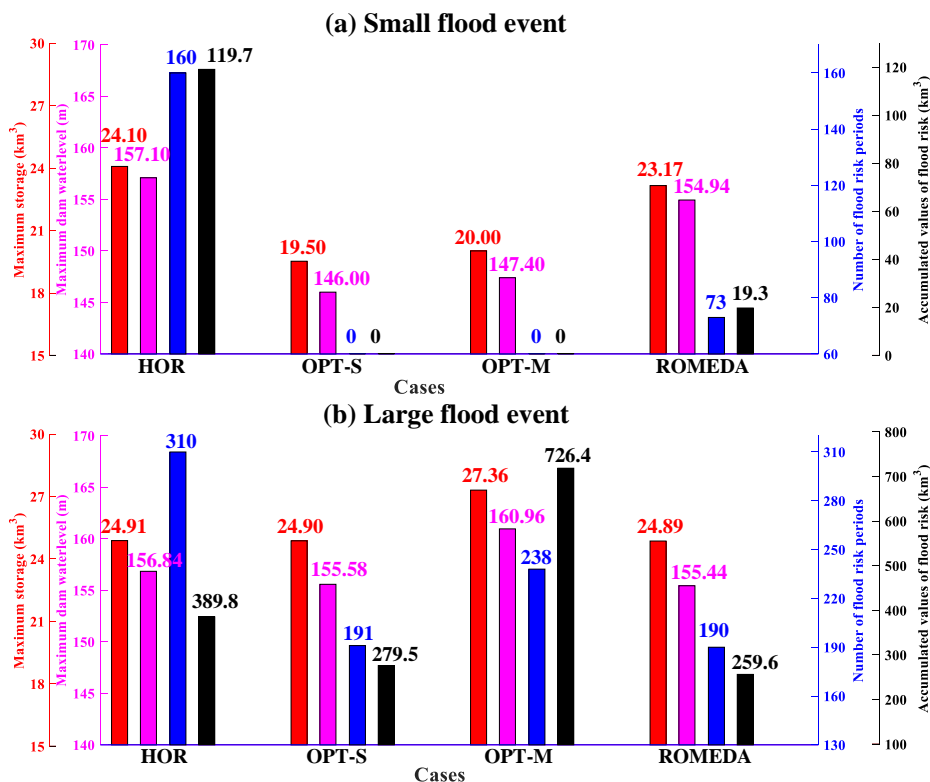
447 as shown in Figure 8b; the maximum release remains 310 time periods (from period 120 to  
448 430), almost half of the total periods. These results indicate that reservoir operators in HOR  
449 behave differently when they deal with small and large flood events. It seems that the reservoir  
450 operators have aggressive behaviors toward the tradeoff between flood control and hydropower  
451 generation during a small flood event, while they are more conservative during a large flood  
452 event by taking quicker and stronger measures for peak-clipping.

#### 453 4.2 Flood risk vs. water use benefit

454 The performance of HOR, OPT-S, OPT-M, and ROMEDA four cases are further  
455 compared in terms of flood risk and water use benefit. Flood risk is triggered when the reservoir  
456 storage exceeds the threshold level. Besides the maximum reservoir storage and maximum  
457 stage in front of the dam, we choose the number of periods with storage over the threshold and  
458 the accumulated value of flood risk over time as two indicators of flood risk. The accumulated  
459 value of flood risk is calculated as the sum of reservoir storage amount exceeding the threshold  
460 level during the entire flood event. Figure 9 shows the comparison of the indicators of HOR,  
461 OPT-S, OPT-M, and ROMEDA under a small and a large flood event.

462

463



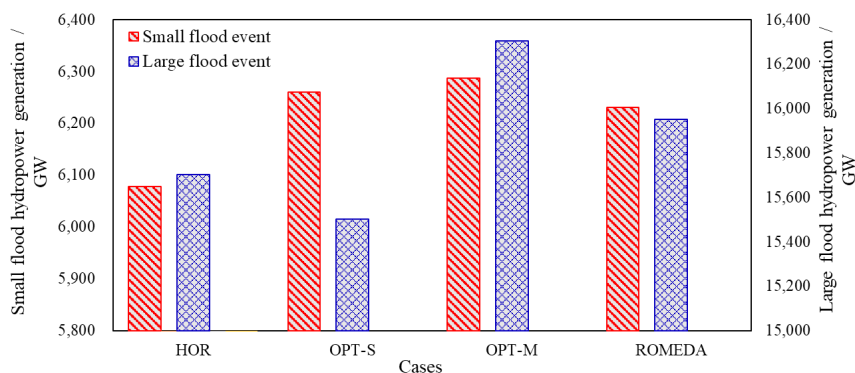
464

465 **Figure 9** Four indicators of flood risk (maximum storage, maximum stage in front of the dam,  
 466 number of flood risk periods, and accumulated values) among HOR, OPT-S, OPT-M, and  
 467 ROMEDA four cases for (a) a small flood event, and (b) a large flood event

468 For the small flood event, OPT-S and OPT-M have the lowest maximum reservoir  
 469 storage and maximum stage in front of the dam, and also have zero risk indicators of flood risk  
 470 periods and accumulated values; ROMEDA has lower values of four indicators than HOR. In  
 471 particular, the risk periods and the accumulated risk (i.e., the sum of reservoir storage amount  
 472 exceeding the threshold level during the entire flood event) are largely reduced under  
 473 ROMEDA. As can be seen in Figure 7c, during some periods, the reservoir storage of  
 474 ROMEDA exceeds but is close to the threshold level.



475 For the large flood event, OPT-M has the largest maximum reservoir storage (27.36  
476 km<sup>3</sup>), maximum stage in front of the dam (160.96 m), and the accumulated value of flood risk  
477 (726.4 km<sup>3</sup>) due to the maximization of hydropower generation in the multi-objective  
478 optimization context. HOR has the largest number of flood risk periods (310 periods). The  
479 performance of OPT-S and ROMEDA are close, but ROMEDA has the lowest values of four  
480 indicators among the four cases, indicating that the conservative behaviors of reservoir  
481 operators as reflected in HOR have an important influence on flood risk reduction with a large  
482 flood event. Thus, the proposed ROMEDA performs well in terms of flood risk reduction by  
483 combining the optimization model results and the experiences of reservoir operators.



484

485 **Figure 10** Hydropower generation comparison among HOR, OPT-S, OPT-M, and ROMEDA  
486 for a small and a large flood event.

487 To further compare the four cases with respect to the reservoir operation purpose  
488 beyond flood control, Figure 10 displays the hydropower generation during a small and a large  
489 flood event given that in the case study reservoir, hydropower is the major objective for the  
490 reservoir operators subject to flood control requirements. As there is a magnitude difference of  
491 inflow between a small and a large flood event, the hydropower generation of the four cases



492 under the small and the large flood event is compared with different scales as shown in Figure  
493 10. As expected, OPT-M has the largest hydropower generation among the four cases given its  
494 multi-objective of flood control and hydropower generation with a small and a large flood  
495 event. OPT-S results in the lowest hydropower generation among the four cases given its sole  
496 objective of flood control in a large flood event. The performance of ROMEDA is between  
497 OPT-M and HOR in a small and a large flood event, i.e. the hydropower generation of  
498 ROMEDA is lower than that of OPT-M but higher than that of HOR. The amount of  
499 hydropower generation depends on release and the hydraulic head (which usually has a  
500 consistent relationship with reservoir storage). As can be seen from Figure 7, for the small  
501 flood event, HOR takes low releases during the first and second flood peak in order to store  
502 water to build a high hydraulic head. While by following the recommendation from the  
503 optimization model, ROMEDA take higher releases than HOR. In general, the situation in a  
504 large flood event is the same as that in a small flood event (Figure 8). Eventually the associated  
505 levels of release and head under ROMEDA results in higher hydropower generation than HOR.  
506 Therefore, compared to ROMEDA, HOR results in a low water use profit and high flood risk  
507 under a small and a large flood event. This implies that the practices of the reservoir operators  
508 can be improved by a model which may respond more closely to the current state of the  
509 reservoir and forecasts of future inflow.



## 510 **5 Discussions**

511           The effects of assimilating real-time observations for modeling error correction, the  
512 form of the objective function, and inflow forecast uncertainty on the performance of  
513 ROMEDA are discussed in this section.

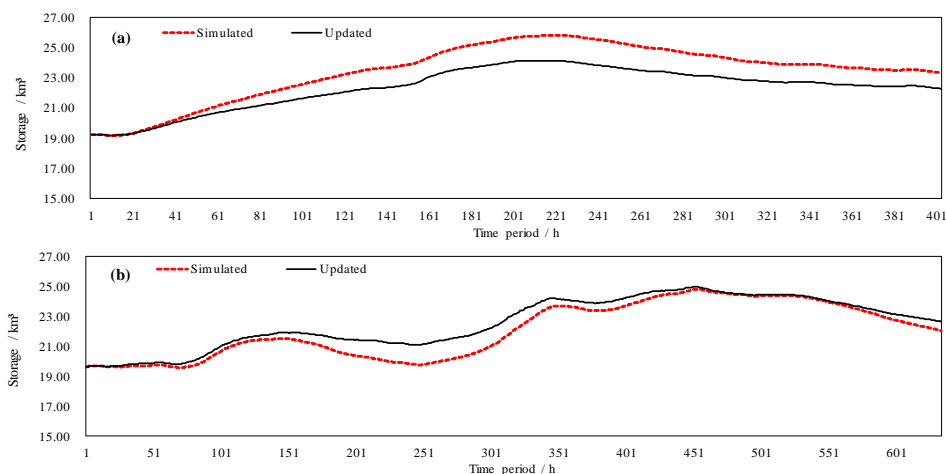
### 514           5. 1 Effects of real-time observations

515           ROMEDA, a human-machine interactive method, utilizes data assimilation to connect  
516 reservoir optimization-simulation models and observations resulting from actual reservoir  
517 releases. Data assimilation of real-time observed stages at different sections along the reservoir  
518 channel can reduce model errors and enhance the accuracy of the unsteady flow routing model.

519           Figure 11 shows the effectiveness of the assimilation of stage observations on  
520 eliminating the model errors on the reservoir storage under HOR by two cases with and without  
521 data assimilation under the small and large flood events. Under one case, the storage is  
522 calculated using the same inputs of historical inflows and releases using the numerical  
523 Preissmann scheme directly (OPT also takes this method); under the other case, the storage is  
524 simulated by the scheme along with the assimilation of stage observations. As shown in Figure  
525 11a, the storage simulated without data assimilation is larger than that with data assimilation,  
526 indicating that for a small flood event, the on-channel reservoir system simulation model may  
527 overestimate the reservoir storage. The overestimated storage may mislead reservoir operators  
528 into paying additional unnecessary attention to flood control, which may result in unnecessary  
529 loss of hydropower generation. However, the opposite result can be seen for a large flood event  
530 in Figure 11b, i.e., the storage simulated without data assimilation is underestimated, which



531 may mislead reservoir operators into underestimating flood risk. This further confirms the  
532 advantage of the data assimilation in ROMEDA method by mitigating modeling errors and  
533 enhancing the effectiveness of the modeling work.



534  
535 **Figure 11** The historical storage difference resulted from the model error for (a) small and (b)  
536 large flood events

## 537 5. 2 On the form of the objective function of OPT

538 An optimization model can always be improved to make it closer to the “idea one”.  
539 However, a realistic way to use a model is to combine the model result with operators’ choices  
540 based on their experiences, knowledge, and behaviors. In this study, flood control is the  
541 primary objective during flooding season, particularly the flood peak period. For the case study  
542 reservoir to test the proposed method, reservoir operators also try to avoid large reduction of  
543 hydro-energy generation. Thus, we set up a single-objective optimization model (OPT-S)  
544 considering flood control and a multi-objective optimization model (OPT-M) considering both  
545 flood control and hydropower generation. Based on the comparison of flood risk and



546 hydropower generation among the four cases (HOR, OPT-S, OPT-M, and ROMEDA) in Figure  
547 9 and 10, we found that OPT-S and OPT-M can both achieve better performance of flood risk  
548 and hydropower generation than HOR and ROMEDA in a small flood event (Figure 9a and  
549 10); while OPT-S has a smaller value of hydropower generation and OPT-M has larger flood  
550 risk indicators than HOR and ROMEDA in a large flood event (Figure 9b and 10). This  
551 indicates that different objective combinations have different performances for flood events  
552 with different magnitudes. However, ROMEDA, which incorporates the  
553 knowledge/experience of reservoir operators and the outputs of the optimization model, can  
554 achieve a good performance of flood risk reduction and hydropower generation in both a small  
555 and a large flood event (Figure 9 and 10). This indicates that ROMEDA makes more effective  
556 use of the reservoir operators' experience and the optimization model.

### 557 5.3 On forecast uncertainty

558 Weather forecast uncertainty is vital to real-time reservoir flood control. The forecast  
559 uncertainty especially with long lead time (Zhao and Zhao, 2014) with climate/weather  
560 variables such as precipitation (Saavedra Valeriano et al., 2010) or hydrologic variable such as  
561 reservoir inflows (Maurer and Lettenmaier, 2004) all have significant impact on real-time  
562 reservoir operation. In this paper, historical inflow is used as "perfect inflow forecast" to test  
563 the proposed method, underlying an assumption that the uncertainty level of the forecasts with  
564 relatively short heading time horizon (72-hour) is low. While the focus of this paper is to  
565 demonstrate the human-machine interactive method, it can be extended to account forecast  
566 uncertainty, for example, by adopting Model Predictive Control (MPC) (Galelli et al., 2014;  
567 Ficchi et al., 2015).





## 568 **6 Conclusions**

569           Reservoir operation models, especially optimization models are usually suitable for  
570 offline analysis, and it is unrealistic to assume the actual reservoir operation can be automatic  
571 based on any modeling results. This paper proposes the Real-time Optimization Model  
572 Enhanced by Data Assimilation (ROMEDA) method to integrate reservoir operators'  
573 justification and optimization modeling results for actual reservoir release decisions during the  
574 flooding season. Reservoir operators can choose when to adopt the modeling results according  
575 to their considerations which vary by person and by reservoir. ROMEDA also combines the  
576 models (optimization model and an unsteady flow routing model) with observed stages of long  
577 and on-channel reservoirs via data assimilation procedures, which update the reservoir storage  
578 (state) for the optimization and simulation models and also mitigate the effect of model and  
579 observation errors.

580           The advantage of ROMEDA method compared to the traditional single/multi-objective  
581 optimization methods (OPT-S and OPT-M) and historical operation records (HOR) is  
582 demonstrated through a case study with an on-channel reservoir. The results show that reservoir  
583 operators perform differently during a small and a large flood event in dealing with the tradeoff  
584 between flood control and hydropower generation. They behave aggressively in taking some  
585 risk in flooding for more hydropower generation during a small flood event, while  
586 conservatively during a large flood event by taking quicker and stronger measures for flood  
587 peak clipping. Such behavior difference is incorporated to ROMEDA, together with stage  
588 observations, for more realistic reservoir release decisions during a flood event. With the case  
589 study reservoir, the ROMEDA method, which integrates the advantages of both machine and



590 human, results in less flood risk than HOR and OPT-M and larger water use (hydropower)  
591 benefit than HOR and OPT-S.

592 Possible future improvements to ROMEDA include a) the real-time reservoir operation  
593 model with stochastic optimization considering inflow forecast uncertainty (with improved  
594 forecast accuracy and lead time); b) the observation data (with enhanced accuracy); c) better  
595 understanding of reservoir operators' real-world decision behaviors and choices. The  
596 ROMEDA method can be easily applied to other real-time operation problems for a joint use  
597 of optimization and data assimilation.

598

599 **Data availability.** All the code and data used in this study can be requested by contacting the  
600 first author Jingwen Zhang at [jingwenz@illinois.edu](mailto:jingwenz@illinois.edu) and/or the corresponding author Ximing  
601 Cai at [xmcai@illinois.edu](mailto:xmcai@illinois.edu).

602

603 **Author contributions.** JWZ and XMC developed the main ideas and implemented the  
604 algorithms of the methods. JWZ and XHL collected the data used in the case study. JWZ,  
605 XMC, XHL, PL and HW prepared the paper.

606

607 **Competing interests.** The authors declare that they have no conflict of interest.



608 **Acknowledgements**

609 This study was supported by the Chinese Ministry of Science and Technology 973 Research  
610 Program (2018YFC0407405), and the Excellent Young Scientist Foundation of the National  
611 Natural Science Foundation of China (51422907, 51822908). The first author would like to  
612 acknowledge the Chinese Scholarship Council (CSC) for supporting her PhD study at the  
613 University of Illinois at Urbana-Champaign (UIUC).

614

615 **References**

- 616 Barker, D. M., Huang, W., Guo, Y.-R., Bourgeois, A., and Xiao, Q.: A three-dimensional variational data  
617 assimilation system for MM5: Implementation and initial results, *Mon. Weather Rev.*, 132, 897-914, 2004.
- 618 Bauser, G., Franssen, H.-J. H., Kaiser, H.-P., Kuhlmann, U., Stauffer, F., and Kinzelbach, W.: Real-time  
619 management of an urban groundwater well field threatened by pollution, *Environ. Sci. Technol.*, 44, 6802-6807,  
620 2010.
- 621 Becker, L., and Yeh, W. W. G.: Optimization of real time operation of a multiple-reservoir system, *Water Resour.*  
622 *Res.*, 10, 1107-1112, 1974.
- 623 Botto, A., Belluco, E., and Camporese, M.: Multi-source data assimilation for physically based hydrological  
624 modeling of an experimental hillslope, *Hydrol. Earth Syst. Sci.*, 22, 4251-4266, 10.5194/hess-22-4251-2018, 2018.
- 625 Camacho, E. F., and Alba, C. B.: *Model predictive control*, Springer Science & Business Media, 2013.
- 626 Carton, J. A., and Giese, B. S.: A reanalysis of ocean climate using Simple Ocean Data Assimilation (SODA),  
627 *Mon. Weather Rev.*, 136, 2999-3017, 2008.
- 628 Castellarin, A., Di Baldassarre, G., Bates, P. D., and Brath, A.: Optimal cross-sectional spacing in Preissmann  
629 scheme 1D hydrodynamic models, *J. Hydraul. Eng.*, 135, 96-105, 2009.
- 630 Chang, and Chang, F. J.: Intelligent control for modelling of real-time reservoir operation, *Hydrol. Process.*, 15,  
631 1621-1634, 10.1002/hyp.226, 2001.
- 632 Chang, Chang, L. C., and Chang, F. J.: Intelligent control for modeling of real-time reservoir operation, part II:  
633 artificial neural network with operating rule curves, *Hydrol. Process.*, 19, 1431-1444, 2005.
- 634 Chu, W. S., and Yeh, W. W.-G.: A nonlinear programming algorithm for real-time hourly reservoir operations, *J*  
635 *Am Water Resour Assoc*, 14, 1048-1063, 10.1111/j.1752-1688.1978.tb02245.x, 1978.
- 636 Crow, W. T., and Loon, E. V.: Impact of Incorrect Model Error Assumptions on the Sequential Assimilation of  
637 Remotely Sensed Surface Soil Moisture, *J. Hydrometeorol.*, 7, 421-432, 10.1175/jhm499.1, 2006.
- 638 Deng, C., Liu, P., Guo, S., Wang, H., and Wang, D.: Estimation of nonfluctuating reservoir inflow from water  
639 level observations using methods based on flow continuity, *J. Hydrol.*, 529, 1198-1210, 2015.
- 640 Ding, W., Zhang, C., Peng, Y., Zeng, R., Zhou, H., and Cai, X.: An analytical framework for flood water  
641 conservation considering forecast uncertainty and acceptable risk, *Water Resour. Res.*, 51, 4702-4726, 2015.
- 642 Draper, A. J.: *Implicit stochastic optimization with limited foresight for reservoir systems*, PhD, University of



- 643 California, Davis, Sacramento, California, 2001.
- 644 Draper, A. J., and Lund, J. R.: Optimal hedging and carryover storage value, *J. Water Res. Plan. Man.*, 130, 83-  
645 87, 2004.
- 646 Dubrovin, T., Jolma, A., and Turunen, E.: Fuzzy model for real-time reservoir operation, *J. Water Res. Plan. Man.*,  
647 128, 66-73, 10.1061/(ASCE)0733-9496(2002)128:1(66), 2002.
- 648 Evensen, G.: Sequential data assimilation with a nonlinear quasi-geostrophic model using Monte Carlo methods  
649 to forecast error statistics, *J. Geophys. Res. [Oceans]* 99, 10143-10162, 1994.
- 650 Feng, M., Liu, P., Guo, S., Shi, L., Deng, C., and Ming, B.: Deriving adaptive operating rules of hydropower  
651 reservoirs using time-varying parameters generated by the EnKF, *Water Resour. Res.*, 53, 6885-6907, 2017.
- 652 Ficchi, A., Raso, L., Dorchie, D., Pianosi, F., Malaterre, P.-O., Van Overloop, P.-J., and Jay-Allemand, M.:  
653 Optimal operation of the multireservoir system in the seine river basin using deterministic and ensemble forecasts,  
654 *J. Water Res. Plan. Man.*, 142, 05015005, 2015.
- 655 Galelli, S., Goedbloed, A., Schwanenberg, D., and van Overloop, P.-J.: Optimal real-time operation of  
656 multipurpose urban reservoirs: case study in Singapore, *J. Water Res. Plan. Man.*, 140, 511-523,  
657 10.1061/(ASCE)WR.1943-5452.0000342, 2014.
- 658 Garcia, C. E., Pretz, D. M., and Morari, M.: Model predictive control: theory and practice—a survey, *Automatica*,  
659 25, 335-348, 1989.
- 660 Gerdt, M.: Optimal control of ODEs and DAEs, Walter de Gruyter, 2012.
- 661 Hejazi, M. I., and Cai, X.: Building more realistic reservoir optimization models using data mining—A case study  
662 of Shelbyville Reservoir, *Adv. Water Resour.*, 34, 701-717, 2011.
- 663 Houtekamer, P. L., and Mitchell, H. L.: Data assimilation using an ensemble Kalman filter technique, *Mon.*  
664 *Weather Rev.*, 126, 796-811, 1998.
- 665 Hsu, N. S., and Wei, C. C.: A multipurpose reservoir real-time operation model for flood control during typhoon  
666 invasion, *J. Hydrol.*, 336, 282-293, 10.1016/j.jhydrol.2007.01.001, 2007.
- 667 Huang, B., Kinter, J. L., and Schopf, P. S.: Ocean data assimilation using intermittent analyses and continuous  
668 model error correction, *Adv. Atmos. Sci.*, 19, 965-992, 10.1007/s00376-002-0059-z, 2002.
- 669 Jahanpour, M., Tolson, B. A., and Mai, J.: PADDs algorithm assessment for biobjective water distribution system  
670 benchmark design problems, *J. Water Res. Plan. Man.*, 144, 04017099, 2018.
- 671 Kanamitsu, M.: Description of the NMC global data assimilation and forecast system, *Weather Forecast*, 4, 335-  
672 342, 1989.
- 673 Liu, Y., and Gupta, H. V.: Uncertainty in hydrologic modeling: Toward an integrated data assimilation framework,  
674 *Water Resour. Res.*, 43, W07401, 2007.
- 675 Macian-Sorribes, H., and Pulido-Velazquez, M.: Inferring efficient operating rules in multireservoir water  
676 resource systems: A review, *Wiley Interdisciplinary Reviews: Water*, n/a, e1400, 10.1002/wat2.1400, 2019.
- 677 Maestre, J., Raso, L., Van Overloop, P., and De Schutter, B.: Distributed tree-based model predictive control on a  
678 drainage water system, *J. Hydroinform.*, 15, 335-347, 2012.
- 679 Maurer, E. P., and Lettenmaier, D. P.: Potential effects of long-lead hydrologic predictability on Missouri River  
680 main-stem reservoirs, *Journal of Climate*, 17, 174-186, 2004.
- 681 Moradkhani, H., Sorooshian, S., Gupta, H. V., and Houser, P. R.: Dual state-parameter estimation of hydrological  
682 models using ensemble Kalman filter, *Adv. Water Resour.*, 28, 135-147, 2005.
- 683 Munier, S., Polebistki, A., Brown, C., Belaud, G., and Lettenmaier, D.: SWOT data assimilation for operational  
684 reservoir management on the upper Niger River Basin, *Water Resour. Res.*, 51, 554-575, 2015.
- 685 Oke, P., Schiller, A., Griffin, D., and Brassington, G.: Ensemble data assimilation for an eddy-resolving ocean  
686 model of the Australian region, *Q. J. Roy. Meteor. Soc.*, 131, 3301-3311, 2005.



- 687 Pan, M., and Wood, E. F.: Data assimilation for estimating the terrestrial water budget using a constrained  
688 ensemble Kalman filter, *J. Hydrometeorol.*, 7, 534-547, 2006.
- 689 Preissmann, A.: Propagation of translatory waves in channels and rivers, Proceedings of the 1st Congress of  
690 French Association for Computation, Grenoble, France, 1961, 433-442,
- 691 Raso, L., Schwanenberg, D., van de Giesen, N., and van Overloop, P.: Short-term optimal operation of water  
692 systems using ensemble forecasts, *Adv. Water Resour.*, 71, 200-208, 2014.
- 693 Reichle, R. H., Crow, W. T., and Keppenne, C. L.: An adaptive ensemble Kalman filter for soil moisture data  
694 assimilation, *Water Resour. Res.*, 44, W03423, 10.1029/2007WR006357, 2008.
- 695 Saavedra Valeriano, O. C., Koike, T., Yang, K., Graf, T., Li, X., Wang, L., and Han, X.: Decision support for dam  
696 release during floods using a distributed biosphere hydrological model driven by quantitative precipitation  
697 forecasts, *Water Resour. Res.*, 46, 2010.
- 698 Soncini-Sessa, R., Weber, E., and Castelletti, A.: Integrated and participatory water resources management-theory,  
699 Elsevier, 2007.
- 700 Tolson, B. A., and Shoemaker, C. A.: Dynamically dimensioned search algorithm for computationally efficient  
701 watershed model calibration, *Water Resour. Res.*, 43, W01413, 10.1029/2005WR004723, 2007.
- 702 Trenberth, K. E., Koike, T., and Onogi, K.: Progress and prospects for reanalysis for weather and climate, *Eos*,  
703 *Transactions American Geophysical Union*, 89, 234-235, 10.1029/2008eo260002, 2008.
- 704 Wang, D., and Cai, X.: Robust data assimilation in hydrological modeling – A comparison of Kalman and H-  
705 infinity filters, *Adv. Water Resour.*, 31, 455-472, 10.1016/j.advwatres.2007.10.001, 2008.
- 706 Wang, D., Chen, Y., and Cai, X.: State and parameter estimation of hydrologic models using the constrained  
707 ensemble Kalman filter, *Water Resour. Res.*, 45, W11416, 2009.
- 708 Xie, X., and Zhang, D.: Data assimilation for distributed hydrological catchment modeling via ensemble Kalman  
709 filter, *Adv. Water Resour.*, 33, 678-690, 2010.
- 710 You, J. Y., and Cai, X.: Hedging rule for reservoir operations: 1. A theoretical analysis, *Water Resour. Res.*, 44,  
711 W01415, 2008.
- 712 Zhao, Q., Cai, X., and Li, Y.: Determining inflow forecast horizon for reservoir operation, *Water Resour. Res.*, 55,  
713 4066-4081, 2019.
- 714 Zhao, T., Yang, D., Cai, X., Zhao, J., and Wang, H.: Identifying effective forecast horizon for real-time reservoir  
715 operation under a limited inflow forecast, *Water Resour. Res.*, 48, 2012.
- 716 Zhao, T., and Zhao, J.: Joint and respective effects of long-and short-term forecast uncertainties on reservoir  
717 operations, *J. Hydrol.*, 517, 83-94, 2014.
- 718